



PDF analysis of PuAl alloys local structure

C. Platteau *, P. Bruckel, B. Ravat, F. Delaunay

CEA Valduc, 21120 Is-sur-Tille, France

A B S T R A C T

For understanding singular properties of plutonium, there is a need in studying the average and local atomic structure in Pu alloys. To study the local structure of the δ phase, a pair distribution function (PDF) analysis was done and has shown some significant differences with the average structure.

© 2008 Elsevier B.V. All rights reserved.

1. Introduction

The delta phase of plutonium is stable between 319 °C and 451 °C but can be held at room temperature by alloying plutonium with delta phase stabilizer elements such as: Al, Ga, Ce and Am. Delta stabilized plutonium alloys are solid solutions where the solute atoms substitute plutonium atoms in the face-centred cubic structure [1–3]. In the solubility range of solutes, the extent of the delta phase stability can be strongly affected by the variation of parameters such as the temperature or the pressure [2,3] leading to martensitic transformation. Moreover, the delta-stabilized Pu alloys have odd physical properties such as changes of the thermal expansion coefficients or increases of the electrical resistivity down to –173 °C. To gain understanding of these properties, it is necessary to study the local atomic structure in the Pu alloys because the physical properties of many complex materials may be related to the local disruption in the atomic arrangement [4,5].

Classical X-ray diffraction suits to describe the average crystal-line structure (long-range order). So when the materials are locally disordered or crystallized in nanostructure, this technique is not adapted to analyze those local arrangements. Conversely, absorption studies by using EXAFS allow to accede to very short-range information (about 8 Å), but the information about 2nd or 3rd neighbours quickly falls off for δ -Pu alloys. Thus, the pair distribution function (PDF) analysis appears as an interesting alternative since this type of analysis gives local information on short and medium range distances [6] and is so well adapted to structural investigations such as the difference of atoms location from their ideal position in the lattice, the presence of nanodomains.

First widely used for the characterization of amorphous and liquid samples [7], the PDF analysis has been extended to the study of crystalline materials owing to the progress in synchrotron sources, pulsed neutron sources and computer technology [6]. Actually, PDF analysis is a total scattering technique that takes into account both Bragg and diffuse scattering and gives information in

the real space on various length scale. The Bragg peaks contain information about the crystal periodicity, namely the long-range order, whereas the diffuse scattering is the result of local atomic displacements from the ideal positions in a perfect crystal. PDF is in fact the reduced pair distribution function $G(r)$ which is defined by the following below equation:

$$G(r) = 4\pi r \rho_0 [g(r) - 1] = \frac{2}{\pi} \int_0^\infty Q [S(Q) - 1] \sin(Qr) dQ, \quad (1)$$

where ρ_0 is the average number density, $g(r)$ is the pair distribution function, r is the distance, Q is the wavevector and $S(Q)$ is the total scattering structure function. The $G(r)$ function has the great advantage to be able to be determined by a direct Fourier Transform from the intensity data without any other information on the material. Moreover, the amplitude of the oscillations gives a direct measure of the structural coherence of the sample.

Thus, the purpose of this work was to characterize the local atomic structure of a δ -stabilized Pu–Al alloy by applying PDF analysis on a total diffuse scattering pattern corresponding to collected data with high-energy X-rays. Details in data collection, PDF calculation and a discussion on the observed differences between local and average structure are developed.

2. Experimental details and data analysis

2.1. Sample preparation

A δ -Pu alloy with a concentration of aluminium of 3 at.% was prepared by hot casting. The cast rod was first cut in plates of 300 μm thick. Subsequent vacuum anneal for 200 h at 450 °C was performed in order to homogenize the distribution of Al atoms [8] and the homogenisation of the sample was confirmed by metallographic observation. An adequate sample with dimensions of 140 μm \times 140 μm \times 100 μm had to be prepared to limit the radioactivity as required by the ESRF. In view of that, the first step of the sample preparation was to cold roll the homogenized plates of 300 μm down to a thickness of 140 μm . But the cold rolling process induced a plastic deformation of the grains of about 53%. Thus, a

* Corresponding author.

E-mail address: platteau.cyril@yahoo.fr (C. Platteau).

heat treatment for 20 h at 450 °C was performed in order to anneal internal stresses that would have been harmful for the further analysis. Afterward, the stress-free plate was electropolished to remove surface oxides as well as other possible impurities at a voltage of 40 V in a cooled bath (90% ethylene glycol and 10% nitric acid) at a temperature of -7°C and cut down to $140 \times 140 \times 100 \mu\text{m}^3$ under a microscope. As a final step, the sample was positioned in specifically designed sample-holder made up of iron–nickel alloy and recovered by two layers of adhesive Kapton foils of $60 \mu\text{m}$ thick to avoid Pu contamination. Handling was done in gloves-boxes under pure argon-atmosphere in order to avoid significant surface re-oxidation after electropolishing. Eventually, the PuAl sample enclosed in the sample-holder was controlled using an α radiation detector to ensure that it was not contaminated with plutonium dust. In addition to PuAl sample, a blank sample and a Si-powder sample were also prepared. The blank sample corresponds to the Fe–Ni sample-holder enclosed between two Kapton foils without PuAl alloy. Its use allowed the scattered signal of the sample-holder to be removed in order to only restrict the PDF analysis to the scattered signal of PuAl alloy. The Si powder was used to accurately determine the wavelength and to calibrate the sample-to-detector distance.

2.2. Data collection

A total X-ray scattering experiment was performed using high-energy X-rays of 88.9 keV ($\lambda = 0.139455 \text{ \AA}$). Measurements were carried out in the flat plate transmission geometry at room temperature and ambient pressure on the ID15B beamline at the ESRF (European Synchrotron Radiation Facility). The wavelength of the incident beam was selected using a monochromator made up of slits. Front slits were used to bring the beam size down to about $100 \mu\text{m}$. The scattered signal was collected using a two-dimensional image-plate detector Mar345. As PDF calculation is a Fourier Transformation of the total scattering function $S(Q)$, the data had to be recorded on an as large as possible Q -range in order to avoid large ripples, which could interfere with the structural information in the PDF. Thus, the high-energy incident beam of 88.9 keV allows to reach a high Q value of about 90 \AA^{-1} . However, the use of the Mar345 detector physically limits the acquisition to $Q_{\text{max}} = 33.7 \text{ \AA}^{-1}$ because the image-plate camera is a round disk with a usable diameter of 345 mm. On the other hand, this detector has the main advantage to allow a data collection with very short counting time and an improvement of the counting statistic (about 5–10 s per image) compared with conventional X-ray detectors [9]. The experiments were performed at three different sample-to-detector distances ($D_{\text{sd}} = 173.637 \text{ mm}$, 443.637 mm and 1143.631 mm). These distances, respectively, correspond to Q -ranges of $3.9\text{--}33.7 \text{ \AA}^{-1}$, $1.9\text{--}16.4 \text{ \AA}^{-1}$, $0.8\text{--}6.6 \text{ \AA}^{-1}$. The highest D_{sd} distance gives accurate information at low Q -range where the most well-defined Debye rings, namely the Bragg's peaks, are observed. The shortest D_{sd} distance allows the diffuse scattering to be col-

lected (high Q -range). The intermediate D_{sd} distance is required for a better accuracy of the three data sets merging during the determination of the experimental PDF. Each measurement was carried out 10 times for the three distances D_{sd} in order to improve the counting statistics. Fig. 1 shows the images obtained for the different sample-to-detector distances.

2.3. PDF extraction

The images collected with the Mar345 detector were first converted into numerical data providing intensities versus scattering angles using the *Fit2D* program [10]. Then, corrections of detector angular tilt, polarization and position of the beam center, were applied. For a given D_{sd} distance, the correction parameters were accurately defined for one image and applied to the other images recorded in the same experimental conditions. Afterward, the intensities files were added and the resulting files corresponding to the three distances D_{sd} of measurement were merged using the *PDFgetX2* program [11] (Fig. 2). Then, the intensity was normalized with respect to the incident flux, namely the monitor counts, measured using the first ion chamber. In order to determine the total scattering structure function $S(Q)$, the most relevant corrections such as the container absorption ('container' refers to the blank sample), the sample self-absorption, the Compton scattering and the Laue diffuse scattering were also applied. Then, the Fourier transformation allowed eventually to lead to the determination of the reduced pair distribution function $G(r)$.

2.4. Classical X-ray diffraction refinement

In order to verify the quality of the diffraction pattern $I = f(2\theta)$, we have performed a classical Rietveld refinement in reciprocal space of the Pu- δ phase with the software FullProf [12]. The preferred orientation function selected is the exponential one: $P_{\text{hkl}} = \exp[G_1 \cdot \alpha_{\text{hkl}}^2]$, where G_1 is an adjustable parameter and α_{hkl} is the angle between the scattering vector and the normal to the crystallites (plate morphology). Table 1 summarizes the refined parameters of the best refinement obtained and the refined pattern is drawn on Fig. 2. This XRD refinement highlights that there is only one crystalline phase that diffracts in our sample (Pu- δ). Furthermore, it has proved that there is only a weak preferred orientation effect as the value of the preferred orientation parameter G_1 is close to 0 ($G_1 = -0.068$), and as the refinement without any preferred orientation leads to similar results (Fig. 2).

2.5. Real space Rietveld refinement

For extracting structural information from the PDF, a real space Rietveld analysis was performed. This approach is similar to the conventional Rietveld refinement and therefore the refined parameters are exactly the same. Nevertheless, the fundamental difference results from the fact that the structural refinement is

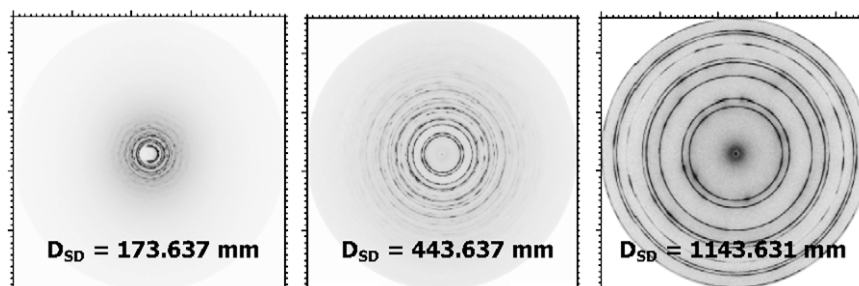


Fig. 1. Images obtained by varying the sample-to-detector distance.

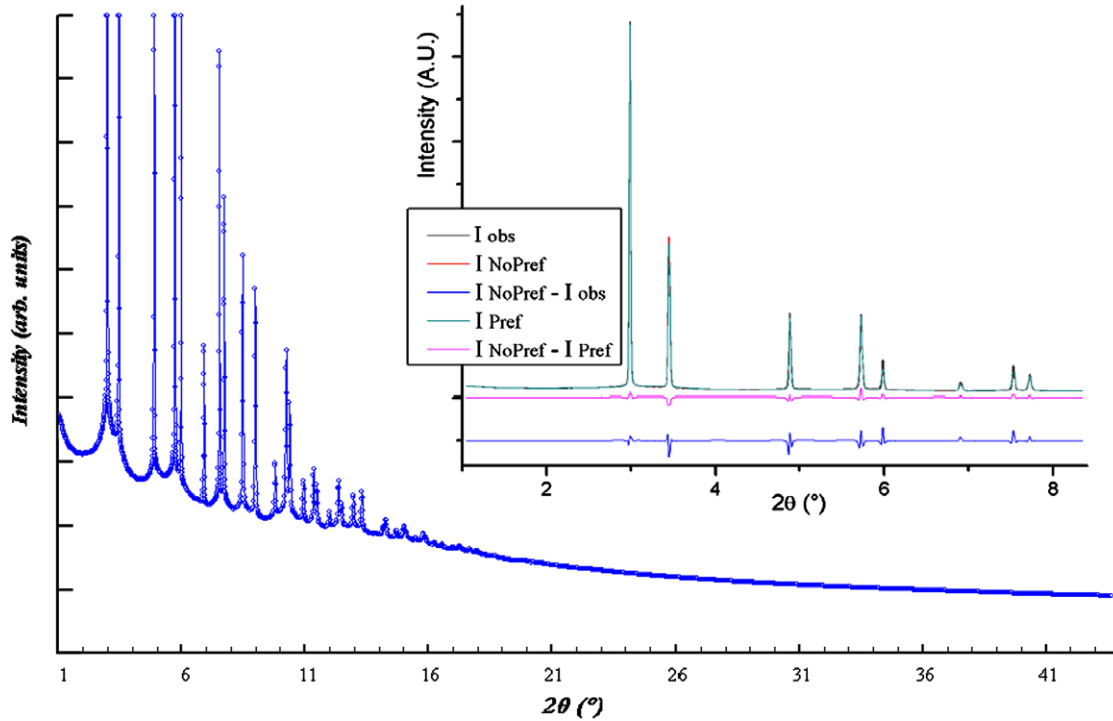


Fig. 2. Merging $I(2\theta)$ of the three data files recorded at different D_{sd} using PDFGetX2 and the comparison between experimental pattern of PuAl3.0% (I_{obs}), the best calculated one (I_{Pref}) and the calculated one without any preferred orientation (I_{NoPref}).

Table 1
Results of the Rietveld refinement.

2 θ fit range: 1.05°–8.30°	$\lambda = 0.139455 \text{ \AA}$	
Agreement factors: $R_{wp} = 4.35\%$	$R_{Bragg} = 0.97\%$	$R_F = 1.04\%$
Cell parameter: $a = 4.6294 (4) \text{ \AA}$	Isotropic Debye-Waller factor: $B_{iso} = 2.07 (15) \text{ \AA}^2$	
Zero point = 0.0027 (5)°	Preferred orientation: $G_1 = -0.068 (4)$ in [001] direction	
Profile parameters (pseudo-Voigt): $U = 0, V = 0.031 (2), W = -0.00029 (5), \eta = 0.13(9), X = 0.029(27)$		

performed on the short-range order namely the local structure which can be slightly different from the average structure. Thus, from a structural model, allowing to calculate the reduced pair distribution function $G(r)$ using the relation (2), a real space Rietveld refinement can be undertaken

$$G_{calc}(r) = \frac{1}{r} \sum_i \sum_j \left[\frac{b_i b_j}{\langle b \rangle^2} \delta(r - r_{ij}) \right] - 4\pi r \rho_0, \quad (2)$$

where r is the distance, b_i the atomic scattering factor of the atom i and ρ_0 the density number. For the real space Rietveld refinement of the studied PuAl alloy PDF the *PDFgui* program was used [13]. Pu atoms were placed in the fcc structure (space group Fm-3m) in accordance with the structure of the δ phase. The refined parameters are the lattice parameter, the scale factor and the isotropic thermal displacement u_{ii} , the linear atomic correlation factor ($\delta 1$), and the Gaussian damping envelope due to limited Q-resolution (Q_{damp}). The results of the real space Rietveld refinement are summarized in Table 2 and the refined PDF is shown in Fig. 3.

Table 2
Results of the real space Rietveld refinement of the PDF of the PuAl sample.

R_{wp}	Fit range	Lattice parameter	$\delta 1$ (atomic correlation)	Q_{damp}	Isotropic thermal displacement u_{ii}
13.52%	2.2–20.0 \AA	4.6151 (16) \AA	1.91 (24)	0.016 (16)	0.0183 (12) \AA^2

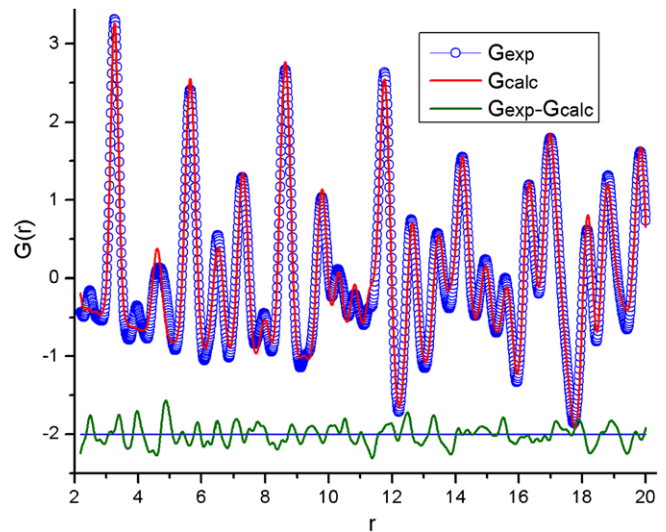


Fig. 3. Fit of the $G(r)$ by the average structure using PDFgui (circles are the extracting PDF from data, solid line is the calculated PDF from model, the difference between the model and the sample is plotted under those curves).

3. Results, discussion and conclusions

A good agreement is found between the experimental PDF of the studied PuAl alloy and the refined PDF calculated from the

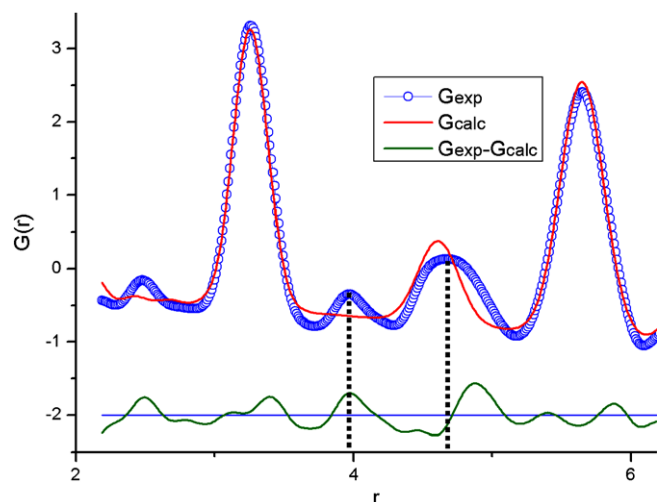


Fig. 4. Fit of the $G(r)$ zoomed at low r .

fcc structure describing the long-range order as observed by X-ray diffraction. Nevertheless, an advanced analysis highlights two differences between the experimental and fitted PDF which arise at low r as shown in Fig. 4. Firstly, the second fcc peak which should be found at 4.618 Å following Ellinger et al. results [14] and corresponding to the [100] direction, is significantly shifted to about 4.70 Å. Furthermore, this peak seems to be able to be split into two distinct peaks. Secondly, an additional peak is observed at a distance $r \sim 4.0$ Å and cannot be attributed to the δ phase of plutonium. Contrary to the ‘peaks’ observed before 2.7 Å which correspond to ripples induced by the Fourier transform, the peaks positioned at 4.0 and 4.7 Å cannot be related to the procedure of the experimental PDF determination. Indeed, different sets of corrections (such as absorption of the sample and the container, Compton scattering, polarization, Q_{\max} of the Fourier Transform, ...) were used without change in amplitude and position of those two differences with the average structure. Furthermore, these observations are not unique to this particular sample, because the same differences were also observed for PuAl alloys with different Al concentrations analyzed in these conditions.

For materials composed of several phases, classical X-ray diffraction can overlook structural phases, notably, these which are non-crystalline, exist in too low amounts, or are organized in nanodomains (even if present in significantly high amounts). In view of that and in order to identify the structure corresponding to the extra peak at $r \sim 4.0$ Å, the opportunity of observing some other plutonium compounds was considered. Thus, to control whether this additional peak could correspond to possible nanostructures of impurities, the structures of Pu surface oxides (PuO_2 , PuO , Pu_2O_3 ...) and intermetallic precipitates (Pu_6Fe ...) [15] were tested using *PDFGui* without any success. Then, tests with different crystalline structure of pure plutonium [16] were performed showing that they did not seem to be able to generate this additional peak. Another hypothesis can be related to EXAFS experiments carried out on delta-stabilized plutonium–gallium alloys by Conradson [1,17]. Indeed, results also showed the presence of extra peaks with the first one at $r \sim 3.8$ Å. This would be the signature of a novel phase – labeled ‘sigma’ by the author – which would coexist with the δ phase for gallium concentrations ranging between 1.70 at.% Ga and 3.35 at.% Ga. The ‘sigma-structure’ was assumed to be a pure plutonium phase and organized in nanodo-

mains allowing no observation using X-ray diffraction. One major debate concerning the existence of the ‘sigma-structure’ is based on the fact that the radius of the PuO_2 second shell is about 3.82 Å that is very close to the position of the extra peak observed for plutonium–gallium alloys [1]. But, according to this work, no PuO_2 oxide was highlighted by total diffuse scattering. Our PDF analysis performed on homogenized PuAl deserve to confirm the observations already done on PuGa but did not allow to interpret the structural differences with the Pu δ phase. A last remark about this extra peak at 4.0 Å is that it is observed both in PuAl and PuGa alloys, and is observed in our PuAl samples with different concentrations of δ stabilizer element, segregated or homogenized. About the broadening of the second fcc peak at about 4.7 Å (Fig. 4), an interpretation would be that this peak is made up of an ordered second coordination shell with an additional peak. This additional peak could be generated by the structure at the origin of the peak at about 4.0 Å. But attempts to found a known structure that generates these two peaks have not yet succeeded.

The PDF analysis has proved his efficiency of revealing, in our PuAl alloys, short-range structural singularities as a complement of the X-ray diffraction and EXAFS. Thus, a possible structural disorder of the second shell in the δ structure of Pu and/or the presence of a nanophase that confirms the observation of a ‘sigma’ phase made on PuGa [1,17] are suggested. In order to complete the real space Rietveld refinement, we propose to use the Reverse Monte-Carlo method (via *RMCPProfile* software [18]) to achieve a structural model which would match with the experimental data. In parallel to the use of this method to analyze the experimental PDF, we plan to continue this work on the future MARS beamline at the synchrotron SOLEIL allowing to access to an X-ray energy of 35 keV. To complete the classical PDF experiment, we propose also to perform a DDF (differential distribution function) [19] experiences, namely a selective PDF around a particular chemical species (Pu or Al).

References

- [1] S.D. Conradson, Los Alamos Science 2 (2000) 356.
- [2] S.S. Hecker, D.R. Harbur, T.G. Zocco, Progress in Materials Sciences 49 (2004) 429.
- [3] S.S. Hecker, Los Alamos Sciences 2 (2000) 290.
- [4] E.S. Bozin, S.J.L. Billinge, H. Takagi, G.H. Kwei, Phys. Rev. Lett. 84 (2000) 5856.
- [5] V. Petkov, I.K. Jeong, J.S. Chung, M.F. Thorpe, S. Kycia, S.J.L. Billinge, Phys. Rev. Lett. 83 (1999) 4089.
- [6] T. Egami, S.J.L. Billinge, Underneath the Bragg peaks: structural analysis of complex materials, in: R.W. Cahn (Ed.), Pergamon Materials Series, Pergamon Press, Elsevier, Oxford, 2003.
- [7] B.E. Warren, X-ray Diffraction, vol. 56, Dover, New York, 1990.
- [8] P. Bruckel, M. Boivineau, B. Ravat, O. Ast, L. Jolly, F. Delaunay, P. Giraud, not yet published.
- [9] P.J. Chupas, X. Qiu, J.C. Hanson, P.L. Lee, C.P. Grey, S.J.L. Billinge, J. Appl. Cryst. 36 (2003) 1342.
- [10] A.P. Hammersley, S.O. Svenson, M. Hanfland, D. Hauserman, High Pressure Research 14 (1996) 235.
- [11] X. Qiu, J.W. Thompson, S.J.L. Billinge, J. Appl. Cryst. 37 (2004) 678.
- [12] J. Rodriguez-Carvajal, M.T. Fernandez-Diaz, J.L. Martinez, J. Phys. Condensed Matter 3 (19) (1991) 3215.
- [13] C.L. Farrow, P. Juhás, J.W. Liu, D. Bryndin, J. Bloch, Th. Proffen, S.J.L. Billinge, J. Phys.: Condens. Matter 19 (2007) 335219.
- [14] F.H. Ellinger, C.C. Land, W.N. Miner, J. of Nuclear Materials 2 (5) (1962) 165.
- [15] R.W.G. Wyckoff, Crystal Structures, second ed., R.E. Krieger Publishing Company Inc., Krieger Drive, Malabar, Florida, 1982.
- [16] W.H. Zachariasen, in: A.S. Coffinberry, W.N. Miner (Eds.), The Metal Plutonium, The University of Chicago, 1961.
- [17] S.D. Conradson, Appl. Spectrosc. 52 (1998) 252A.
- [18] M.G. Tucker, D.A. Keen, M.T. Dove, A.L. Goodwin, Q. Hui, J. Phys.: Condens. Matter 19 (2007) 335218.
- [19] P.H. Fuoss, P. Eisenberger, W.K. Warburton, A. Bienenstock, Phys. Rev. Lett. 46 (1981) 1537.